Application of Plastics CAE: Focusing on Impact Analysis

Sumitomo Chemical Co., Ltd.
Plastics Technical Center
Masaaki Tsutsubuchi
Tomoo Hirota
Yasuhito Niwa
Tai Shimasaki

To review recent topics on impact analysis in the field of plastics, this report outlines the application trends and analysis techniques followed by an explanation of the characteristic physical properties of resins which may be the key points for their practical application. First we introduce how we predict yield stress under a wide range of temperatures and strain rates. Second, for the elastic-plastic model, we explain that it may be appropriate to consider dependence of yield stress on stress state and volume increase due to craze generation. Finally, we show how fracture behavior depends on temperature and strain rate.

This paper is translated from R&D Report, "SUMITOMO KAGAKU", vol. 2011-Ⅱ.

Introduction

It is said that CAE (Computer Aided Engineering) was advocated by Dr. Jason R. Lemon as a concept of using computers widely in designing and developing products sometime before 1980.[1] Since then the concept has become disseminated along with the advancement of computers.

The common challenges faced by each manufacturing industry include reducing the length of the development period for each product, limiting the costs of development and manufacturing, the improvement of product quality and performance, and the mitigation of issues concerning safety and the environment. CAE is used as one of the basic engineering technologies to address such challenges.[2] In the field of plastics, CAE has been widely used for mold and product designs and other purposes. The particular CAE used in the field of plastics is called plastics CAE.

Since 1981, when the term "CAE" emerged, Sumitomo Chemical has made the most of CAE and has engaged in the examination of performance and processability of plastic structures.[3)-6)] Regarding the former, Sumitomo Chemical initially investigated the deformation properties and the vibration and sound properties of plastic structures. The company later broadened the study area to the impact properties, and today we remain involved in that effort. Regarding the latter, Sumitomo Chemical has mainly investigated in the field of injection molding and related areas.[7), 8)] Currently, the company is also investigating the application of CAE to the field of extrusion molding.[9)]

Regarding vibration and sound analysis, Sumitomo Chemical also conducts experiments using a shaker with a temperature and humidity test chamber and a semi-anechoic chamber (**Fig. 1** (a)). Furthermore, for impact analysis we measure the tensile properties under high-speed conditions using a high-speed tensile testing machine, and verify the CAE analysis results via a service test using an impact testing machine (**Fig. 1** (b)).

(a) Semi-anechoic chamber

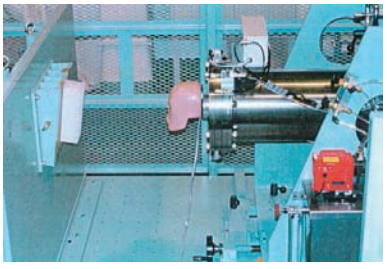

(b) Impact testing machine

Fig. 1 Experimental facilities for Plastics CAE

As CAO (Computer Aided Optimization) advanced toward commercialization, which occurred in or about the year 2000, Sumitomo Chemical examined the application of CAO to plastics CAE and reported on its usefulness.[2] CAO is a form of design automation, optimization and integration technology using computers. It facilitates a significant reduction in and optimization of development periods for plastic products, and improved quality and performance of such products.

In the conventional plastics CAE, the material properties were first input to the system, after which the results regarding the product's performance and processability were obtained. However, Sumitomo Chemical is now also undertaking study with a focus on obtaining the material properties of plastic products based on their polymer structures and resin compositions.[10] We refer to the former method as "CAE for product design" and the latter method as "CAE for polymer design" (**Fig. 2**).

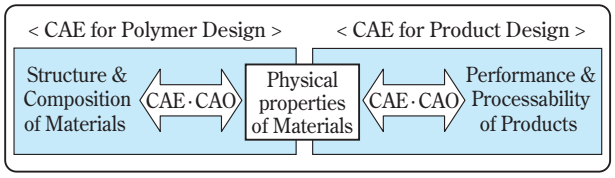

* CAE: Computer Aided Engineering
CAO: Computer Aided Optimization

Fig. 2 Plastics CAE system

This report outlines the CAE application trends and analysis techniques followed by an explanation of the characteristic physical properties of resins which may be the key points for their practical application.

Furthermore, the paper will briefly describe the current application status of impact analysis at Sumitomo Chemical.

Impact Analysis

1. Trends in the Application of Impact Analysis in the Field of Resins

Impact analysis is the simulation of a phenomenon that generates an impact load. It has been used in predicting the crash performance of automobiles, vessels, aircrafts and other vehicles. Examples of the application of impact analysis in the field of resins include investigations into the crash performance of automobile plastic parts, the impact resistance of mobile devices such as cellular phones when they are dropped, as well as the impact properties of sports equipment such as golf clubs and tennis rackets.

Examples of the application of impact analysis of automobile plastic parts include interior parts such as door trims and pillar garnishes installed on pillars around doors and instrument panels located in front of driver seats, as well as exterior parts such as bumper covers.

These plastic parts do not have to possess great strength, but high impact absorbing performance in order to prevent the occurrence of injury to a human body at the time of a collision is often demanded for the protection of occupants and pedestrians. In response to such demands, the impact absorbing performance requirement of a resin part may occasionally be satisfied by adjusting its rigidity using the rib structure or boss structure. In these methods, part design is made more efficient through the use of impact analysis.[11)–16)]

Moreover, regarding instrument panels, because it is necessary to predict the crash performance in combination with air conditioning and/or car audio systems, impact analysis of them in assembled state is also examined.[17)]

Regarding resin materials, properties such as yield stress may change significantly according to the deformation rate. Therefore, a material model designed in consideration of the strain-rate dependency in the relationship between stress and strain is used.[18), 19)] Moreover, because the deformation behavior after failure may greatly affect the part's energy absorption mechanism, analysis using a failure model is also conducted depending on the part involved.[20)–23)] Furthermore, in an impact analysis that takes into account the protection of pedestrians and so on, it is necessary to precisely predict the reaction force of the part demonstrated when the deformation of the resin part recovers after crashing. Therefore, in some cases a change in the recoverability according to the deformation is modeled as a change in the elastic modulus at the time of recovering.[24), 25)]

Additionally, in automobile parts there are cases in which impact analysis has been used to investigate the deployment behavior of the plastic airbag covers in which the airbags are stored. In some such cases, taking into account the temperature (–40°C - 90°C) and the strain-rate dependency of the material, analyses are

conducted using the strain at failure as the failure criterion.[26)]

For a drop-test analysis of mobile devices a study is conducted with the purpose of evaluating a phenomenon that occurs in an extremely short period of time that cannot be fully understood by a mere experiment. Through this study the impact load and strain applied to the housing and printed circuit board immediately after the collision can be evaluated with high precision without considering the strain-rate dependency and/or failure criterion.[27)–29)]

During impact analysis on sports equipment, impact phenomena between the equipment and a ball is studied. While in some cases a simple linear elastic material is used as the material model for sports equipment,[30)] the model in which repulsion behavior can be accurately analyzed is used for balls. For instance, a hyperelastic material model[31), 32)] designed in consideration of the viscoelastic behavior[33)] is used to examine solid golf balls, and for hollow tennis balls a model designed in consideration of the state equation for air in the balls or other similar models is used.[34)]

2. Overview of Analysis Techniques

The authors of this paper mainly use the commercial software LS-DYNA® for impact analysis. LS-DYNA® was released to the market in 1987, and had been developed based on DYNA3D, which was developed by the Lawrence Livermore National Laboratory in 1976.

The analysis techniques with which to evaluate the deformation, strain and stress that occur in structures when external forces are applied are referred to collectively as structural analysis. Within structural analysis, a technique particularly used to analyze the phenomenon whereby a material receives an impact load is called impact analysis. The governing equations of structural analysis are an equation of the equilibrium of force (the equation of motion when taking acceleration into account), a compatibility equation that expresses the continuity of strain, and a constitutive equation that expresses the relationship between stress and strain. All of these are differential equations in time and space coordinates.

In structural analysis differential equations are converted to algebraic equations that can be processed by a computer through the division of continuous time and space (discretization), and the obtained pluralistic simultaneous equations are then calculated numerically. The finite element method is mainly used for the discretization of space in differential equations, and the finite difference method is used for the discretization of time.

(1) Implicit and Explicit Methods

The time discretization method can be classified into two types: an implicit method and an explicit method. While in the latter method the variables at the target time (deformation, strain, stress, etc.) can be calculated using variables at the time immediately before the target time, in the former method it is necessary to solve simultaneous equations containing both variables at the target time and the time immediately before the target time. The number of simultaneous equations with discretized governing equations can often be enormous. Generally, the explicit method, which does not require the numeric calculation of simultaneous equations, is much faster than the implicit method for the calculation of specific time. Because the time that must be considered is short in the context of impact analysis, the explicit method is often applied.

However, in the explicit method it is necessary to fulfill the requirement needed to acquire a numerically stable solution. This condition (requirement) is called the Courant condition. Equation (1) shows the Courant condition of one-dimensional space.

$$C = \frac{u \cdot \Delta t}{\Delta x} \leq 1 \qquad (1)$$

Here, C represents the Courant number, u represents the speed of sound, Δt represents the time step, and Δx represents the space interval.

Furthermore, because $u = \sqrt{E/\rho}$ when u represents the speed of sound, ρ represents the density and E represents Young's modulus, equation (1) can be modified to equation (2).

$$\Delta t \leq \Delta x \sqrt{\rho / E} \qquad (2)$$

Assuming that the subject material is polypropylene, when E = 1.5GPa, ρ = 900kg/m^3 and Δx = 0.001m, then $\Delta t \leq 0.77$ microsecond, thus showing that Δt is an extremely small value. For cases in which the effect of a shock wave is small, then mass scaling, in which the time step is expanded by enlarging the density in the calculation, is used. However, when calculating a fracture event, because it can be considered that the shock wave has a significant effect in many cases, it is necessary to apply mass scaling with extra caution.

Contrastingly, in the implicit method, the time step can be expanded to some extent because the implicit method is not bound by the Courant condition. Once massively parallel computing is disseminated, the use of the implicit method may also be more beneficial in terms of computation time for impact analysis. However, the application of the implicit method can only be seen in a few cases [35].

Although the LS-DYNA® software was originally dedicated to the explicit method, it can now perform calculations using the implicit method as well.

(2) Solid and Shell Models

For the discretization of space in the finite element method, the target shape is divided into several simple shapes. When discretizing space in a faithful manner, target-shape modeling is conducted using a solid element such as a hexahedron or tetrahedron. Such a model is called a solid model. The points used for the discretization of space, i.e., the vertices of the element will be hereinafter referred to as the discretization points.

Resin parts comprise combinations of plate-like shapes, and their thickness is often smaller than their length and width. Therefore, the process of the discretization in the thickness direction of space is often omitted, and in many cases the target shape is modeled using a plane element such as a triangle or quadrilateral. Such a model is called a shell model. Because in a shell model the thickness is defined not by the shape of the model but by the numeric value, the number of discretization points can be reduced, thus reducing the computation load. Additionally, a shell model is usually created on a neutral plane (the middle surface in the thickness direction).

In the explicit method when space is discretized in the thickness direction using a solid model in a tabular shape, the element dimension in the thickness direction will be small, thus reducing the Δx value of equation (1) and resulting in smaller time steps. By using a shell model, the reduction of time steps can be suppressed because there is no need to consider the Courant condition in the thickness direction.

However, in cases that cannot be expressed merely by combining several tabular shapes or cases in which the discretization points that were present on a section perpendicular to a neutral plane before deformation move elsewhere after the deformation, a shell model cannot be used and it is therefore necessary to use a solid model. Impact analysis in falling weight impact tests, as described later in this paper, come under the latter case.

(3) Fluid-Structure Interaction (FSI) Analysis

In the field of impact analysis, fluid-structure interaction (FSI) analysis is popularly conducted.

In continuum mechanics, substances are treated as collections of continuous points (material point). In structural analysis the material point is often used as a discretization point. This is called the Lagrange method. In the Lagrange method the discretization point moves as deformation occurs. On the contrary, in fluid analysis the discretization point is often fixed at a specific position in space. This is called the Euler method.

The Arbitrary Lagrangian-Eulerian (ALE) method is a method in which the discretization point is matched neither to the material point nor to a specific position in space, but is set arbitrarily. The ALE method is occasionally used to successively set the calculating area of a fluid based on the deformation that occurs on the boundary face between the fluid and the structure or on the fluid surface.

FSI analysis considers the interaction between the fluid pressure and deformation of the structure. Normally, a fluid is calculated using either the Euler method or the ALE method, and a structure is calculated using the Lagrange method. Consequently, the fluid and the structure are coupled at the boundary.

3. Characteristics of Material Properties

Cases studied with a focus on polypropylene based resin will be introduced below. Regarding the measurement results described in this paper, stress and strain are nominal values unless otherwise described, and the strain rate is a nominal value calculated based on the setting speed of the test apparatus.

(1) Deformation Behavior

While the material properties of resin change according to the strain rate, the strain-rate dependency of the tensile property is considered scalable through the use of equation (3).[36]

$$\frac{\sigma_2}{\sigma_1}=\left(\frac{\dot{\varepsilon}_2}{\dot{\varepsilon}_1}\right)^n,\ \frac{\varepsilon_2}{\varepsilon_1}=\left(\frac{\dot{\varepsilon}_2}{\dot{\varepsilon}_1}\right)^{-n} \quad (3)$$

Here, σ_1 and σ_2 represent the stress, ε_1 and ε_2 represent the strain, $\dot{\varepsilon}_1$ and $\dot{\varepsilon}_2$ represent the strain rate, and n rep-

resents a constant. Moreover, the subscripted letters represent measurement conditions.

Fig. 3 depicts the results of scaling conducted assuming that the equation can be valid for the relationship between the nominal stress and nominal strain. As for the grade used in this study we could scale the stress-strain relationship under strain rate conditions of approximately $0.5s^{-1}$ or more through the use of equation (3).

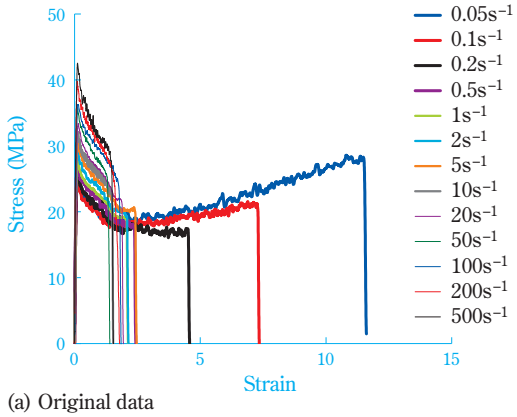

(a) Original data

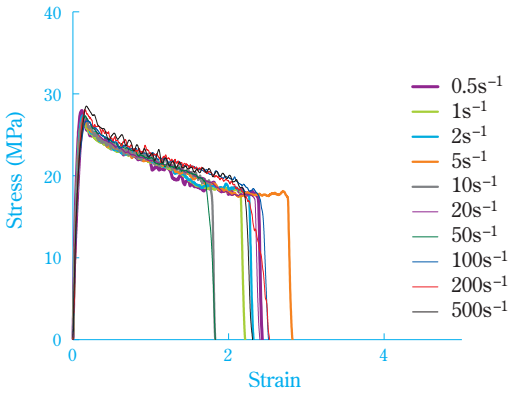

(b) Superposed data by the scaling rule

Fig. 3 Tensile testing results: Relationship between nominal stress and nominal strain

We also surmise that the use of equation (4)[37] will readily smoothen the tensile testing data.

$$\sigma(\varepsilon,\dot{\varepsilon},\theta) = E_0(\dot{\varepsilon},\theta)\frac{1}{w(\dot{\varepsilon},\theta)}\left[1-e^{-w(\dot{\varepsilon},\theta)\varepsilon}\right]e^{h(\dot{\varepsilon},\theta)\varepsilon^2} \quad (4)$$

Here, σ represents the stress, θ represents the temperature, ε represents the strain, $\dot{\varepsilon}$ represents the strain rate, E_0 represents the elastic modulus, w represents the viscoelastic coefficient and h represents the strain hardening coefficient.

Because equation (4) can be used to express the relationship between true stress and true strain, the measurement data described in **Fig. 3** will be used after converting it to the true stress-true strain relationship. The data described in **Fig. 3** (a) can be expressed through equation (4) by appropriately determining E_0, w and h in the areas having a moderate strain level when the strain rate or the temperature is changed.

(2) Elastic-Plastic Model

Normally, crystalline resins demonstrate extremely complicated behavior because they form a mixture of crystals and amorphous material.[38] However, in the current situation it is favorable to use approximate expressions due to the lack of a constitutive equation with which to model their behavior as a mixture, as well as technical issues such as computation time and measurement time for material properties. For this reason an elastic-plastic model has often been used for crystalline resin materials as well as for metallic materials.

(i) Strain Rate and Temperature Dependencies of Yield Stress

When external force is applied to an object, the characteristic of the object whereby it completely recovers its original state after removing the external force is called elasticity. In contrast, the characteristic of the object that retains permanent deformation even after removing the external force is called plasticity. The stress that causes plastic deformation is called yield stress.

In an elastic-plastic model, elasticity is defined by when the stress is less than the yield stress, and plasticity is defined by when the stress exceeds the yield stress.

Although the authors of this paper have normally treated elasticity as linear elasticity (with stress and strain being proportional), we have focused on the strain-rate dependency of the yield stress in impact analysis because the resin material properties showed a significant strain-rate dependency.

When examining the strain-rate dependency of yield stress, the Cowper-Symonds equation (equation (5)) has been conventionally applied. However, it was difficult to improve the accuracy of the strain-rate dependency with this method due to limitations in the range of the measurement speed.

$$\sigma_y = \sigma_{0y}\left[1+(\dot{\varepsilon}/C)^{1/p}\right] \quad (5)$$

Here, σ_y represents the yield stress, σ_{0y} represents the static yield stress, $\dot{\varepsilon}$ represents the strain rate and C and p represent material constants.

In the meantime, equation (6), which is based on the Eyring theory, can express the yield stress as a function of the temperature and strain rate.[39] The yield phenomenon can be expressed using the Eyring theory of nonlinear flow. The Eyring theory of nonlinear flow is one in which stress causes the potential energy barrier of the flow to become asymmetrical (activated), thereby causing the material to flow in a particular direction. When this occurs it can be surmised that the potential energy barrier of the flow at the upstream side is increased by $V_p^*\sigma_y$ and that at the downstream side it is reduced by $V_p^*\sigma_y$. Two activation processes are taken into account in equation (6), and it is considered that the equation is valid for PC, PMMA and PP.

$$\frac{\sigma_y}{T}=\sum_{p=\alpha,\beta}\frac{R}{V_p^*}\sinh^{-1}\left(\frac{\dot{\varepsilon}}{\dot{\varepsilon}_{0,p}^*}\right)$$
$$\dot{\varepsilon}_{0,p}^*=\dot{\varepsilon}_{0,p}\exp\left(-\frac{\Delta U_p}{RT}\right) \quad (6)$$

Here, σ_y represents the yield stress, $\dot{\varepsilon}$ represents the strain rate, $\dot{\varepsilon}_{0,p}$ represents a rate constant, T represents the temperature, R represents the gas constant, V_p^* represents the activation volume and ΔU_p represents the activation energy.

Fig. 4 shows the results of the regression of yield stress using equation (6) toward the results of tensile testing under various rates and temperatures. Furthermore, in **Fig. 4** the strain rates were calculated, taking into account changes in the tensile rate that may occur during the testing process. Using equation (6) enabled us to estimate the yield stress in broader ranges of temperature and strain-rate conditions.

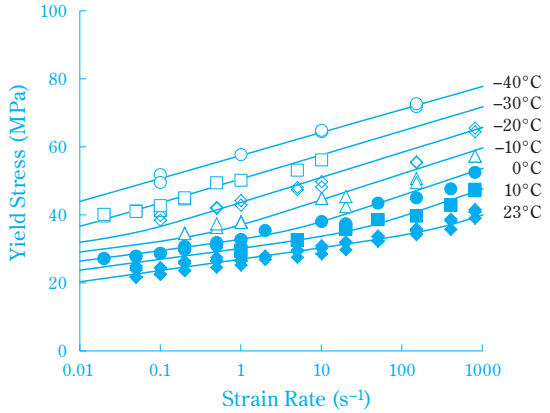

Plots: Experimental data
Curves: Eq.6

Fig. 4 Dependence of yield nominal stress on temperature and nominal strain rate

(ii) Yield Criterion

The von Mises yield criterion, which is most often applied for metal materials, has been defined as shown in equation (7), taking advantage of the fact that the yield stress of metal materials does not depend much at all on hydrostatic pressure (yielding occurs when the second invariant of the deviatoric stress exceeds the yield stress). In terms of physics, the von Mises yield criterion denotes the stress that causes the shear strain energy of each unit volume to exceed its limit. It is therefore surmised that materials do not yield under the condition of being affected only by hydrostatic pressure.

$$\frac{1}{2}\{(\sigma_{xx}-\sigma_{yy})^2+(\sigma_{yy}-\sigma_{zz})^2+(\sigma_{zz}-\sigma_{xx})^2+6(\tau_{xy}^2+\tau_{yz}^2+\tau_{zx}^2)\}\geq\sigma_y^2 \quad (7)$$

Here, σ_y represents the yield stress, σ_{xx}, σ_{yy} and σ_{zz} represent the components of normal stress, and τ_{xy}, τ_{yz} and τ_{zx} represents the components of shear stress.

However, because resin materials possess a "hydrostatic pressure dependency,"[40] which affects the yield condition according to the differences in stress states such as uni- or bi-axial tension, compression and shear, the accuracy of an analysis may not always be adequate when applying the von Mises criterion, which does not depend on hydrostatic pressure.

Thus a material model that can define a complicated yield surface in consideration of stress conditions such as uni- or bi-axial tension, compression and shear, even though it is based on an elastic-plastic model, has garnered attention in recent years because it is expected that such a model can express complex characteristics of resin materials as accurately as possible.[25] In this material model the effect of voids contained in the craze, which occurs after the yield point is reached, can be considered. When voids occur, the material volume will increase, and the stress will decrease at the same time. The former can be defined as plastic Poisson's ratio and the latter can be defined as a damage function, both being defined as functions of plastic strain.

(iii) Plastic Poisson's Ratio and Damage Function

To investigate Poisson's ratio during plastic deformation, the relationship between true strain in the tensile

direction (longitudinal strain, ε_L) and that which is perpendicular to the tensile direction (transverse strain, ε_T), both of which occurred during the tensile test, was measured through image analysis (**Fig. 5**). Poisson's ratio, whose definition had been expanded to a large deformation region ($-d\ \varepsilon_T/d\ \varepsilon_L$, the value obtained by taking the negative of the slope shown in **Fig. 5**), decreased significantly in the region, where it appeared to be immediately after entering the plastic region. This behavior is the same as that seen in the measurement example utilizing the digital image correction method (DICM).[41] However, as shown in **Fig. 5**, there was an observed tendency toward an increase in Poisson's ratio as the strain became larger. Moreover, as described in the literature,[42] it suggested that the strain-rate dependency of Poisson's ratio was minimal.

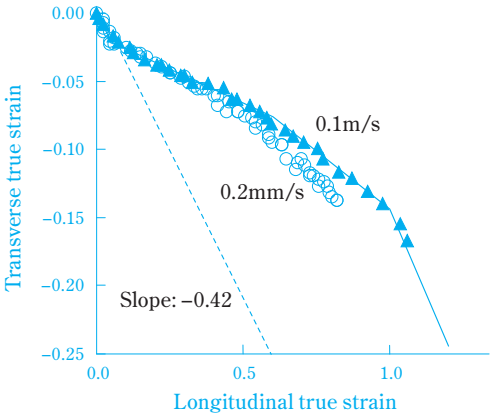

Parallel part length of the specimen: 57mm

Fig. 5 Relationship between transverse true strain and longitudinal true strain

It can be assumed that the phenomenon whereby Poisson's ratio becomes smaller in the plastic region was caused by the volume increase of the specimen (i.e. the decrease in the material width was minimal), which occurred due to the progress of deformation during the occurrence of crazing.[43]

Plastic Poisson's ratio is defined as the value obtained during a tensile test by taking the negative of the ratio between the component of the plastic strain rate perpendicular to the tensile direction ($\dot{\varepsilon}_{pT}$) and that in the tensile direction ($\dot{\varepsilon}_{pL}$) ($-\dot{\varepsilon}_{pT}/\dot{\varepsilon}_{pL}$). However, it was assumed that the difference between plastic Poisson's ratio and Poisson's ratio obtained in the plastic region described above was minimal.

In the conventional elastic-plastic model plastic Poisson's ratio was often determined to be 0.5, assuming that the volume was invariable during plastic deformation. However, it is presumed to be better to take into account the characteristic of resin materials whereby they possess a small plastic Poisson's ratio.

Assuming that the volume which increased during an object's deformation process was equivalent to that of the voids that occurred during the deformation, the damage function was estimated as follows: In **Fig. 6**, assume that when the tensile force F was applied to a rectangular parallelepiped in the vertical direction, the apparent area of the surface perpendicular to the tensile direction was S. Because the apparent area S contains the area of voids S_v, the relationship between the stress σ_d (in consideration of occurrence of voids) and stress σ_p (which is applied to the material itself) can be expressed as equation (8).

$$F = \sigma_d \times S = \sigma_p \times (S - S_v) \tag{8}$$

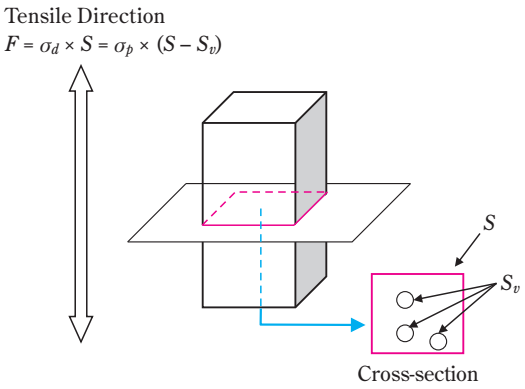

Fig. 6 Stress of damaged material

Given the fact that the ratio between the area of the material and the apparent area is equivalent to the ratio between the volume of the material and the apparent volume, the damage function d can be calculated through equation (9)[44] using the volume increment ΔV and initial volume V_0 since the volume of the material itself does not change.

$$d = 1 - \sigma_d/\sigma_p = 1 - (S - S_v)/S = 1 - 1/(1 + \Delta V/V_0) \tag{9}$$

Furthermore, by estimating the value of the damage function from a change in the apparent volume based on plastic Poisson's ratio, the relationship between the value of the damage function and the plastic strain can be obtained.

(3) Fracture Behavior

In a tensile test using polypropylene based resin, the relationship between the nominal strain at break and the strain rate was roughly obtained using the poly-linear approximation (**Fig. 7**). Subsequently, linear areas were determined as regions A to D in the order of higher rate to lower rate, and the deformation status of each region at the time of fracturing was investigated. As a result, these statuses were classified in association with the phenomenon called "necking," in that a partial constriction occurred in one specimen during the tensile test (**Table 1**).

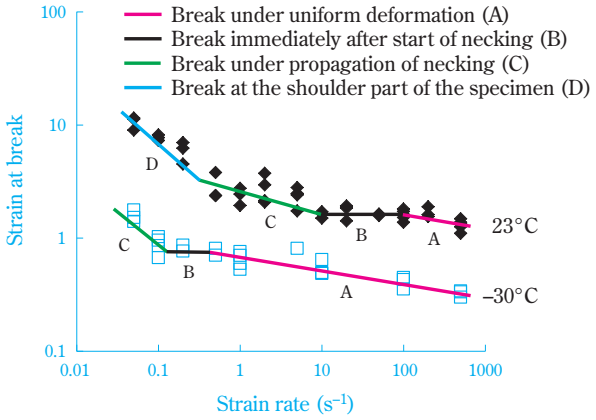

Fig. 7 Relationship between nominal strain at break and nominal strain rate

Table 1 Break behavior of the specimen at tensile testing

Region	Break behavior	Temperature	Nominal strain rate
A	Break under uniform deformation	Low	High
B	Break immediately after start of necking	↓	↓
C	Break under propagation of necking	↓	↓
D	Break at the shoulder part of the specimen	High	Low

Regarding the specimen that fractured prior to the occurrence of necking (region A), we observed almost exactly the same slope for all temperatures in the double-logarithmic plot. Accordingly, the test results were organized by moving data at the lower-temperature side to the higher-rate side and data at the higher-temperature side to the lower-rate side and then superimposing such data onto the data measured at –10°C (**Fig. 8**).

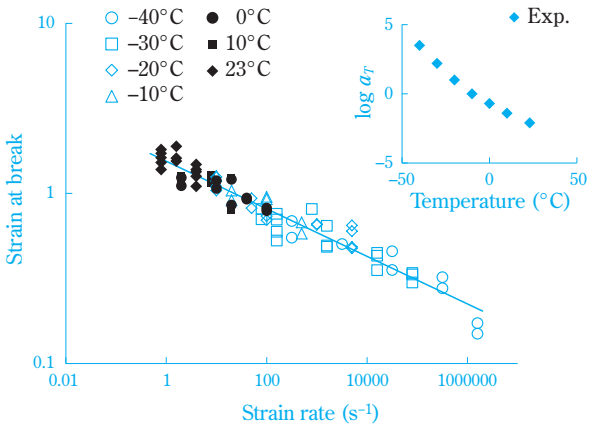

Fig. 8 Results of time-temperature superposition in region A

It has been demonstrated that the time-temperature shift factor (a_T) regarding the fracture characteristics of polyethylene conforms to the WLF equation (10).[45] It is surmised that the time-temperature superposition principle may also be applied to this system.

$$\log a_T = \frac{C_1 (T - T_{ref})}{C_2 + (T - T_{ref})} \qquad (10)$$

Here, T represents the temperature, T_{ref} represents the reference temperature and C_1 and C_2 represent constants.

When comparing using a temperature of 23°C, while the nominal strain at the yield point was approximately 0.2, that at the time of fracturing prior to the start of necking was 1 or greater (**Fig. 7**), thus showing a significant difference between the yield point and the necking starting point. Moreover, no significant change was observed in the width of the parallel part between the yield point and the necking starting point. This fact, together with the whitening of the specimen, suggests the occurrence of crazing. It can be surmised that crazing plays an important role in ductile fracture.

Based on the above examination results, the authors obtained the relationship between plastic strain at failure and the strain rate under the conditions of rate and temperature at which the specimen would fracture after yielding and before the occurrence of necking. Such obtained data is often used for prediction of the fracture behavior of specimens during impact analysis. The authors assume that it is desirable to combine other methods such as image analysis in order to predict the fracture behavior with even greater accuracy.

Shizawa et al., meanwhile conducted a failure prediction test using an elastoviscoplastic constitutive equa-

tion with a craze effect.[46] Craze has been modeled as the phenomenon with the following characteristics: It increases as plastic strain increases; the lower the strain rate is, the greater its propagation rate becomes; and it stops propagating at the oriented molecular region. It has been reported that the above method has enabled the reproduction of the phenomenon whereby the concentrated craze region on the shear band (the region where strain is linearly localized) propagates toward the tensile direction along with the propagation of a constriction as the craze density increases, thereby enabling the prediction of the fracture along the shear band, which may occur at the front edge region of the propagating neck.

4. Examples of Impact Analysis Conducted at Sumitomo Chemical

Applications of impact analysis that has been conducted since the early 1990s will be outlined here. Impact resistance is often demanded in automobile parts and consumer electronics components. Particularly for automobile parts, energy-absorption capability is stipulated by the laws and regulations of many countries in order to protect drivers and passengers. Because energy absorption capability is dependent on both the part shape and material properties, it is ideal to be able to predict the part performance taking both of the above factors into account through the use of plastics CAE.

(1) Impact Analysis on Structures

Initially, Sumitomo Chemical applied the impact analysis mainly with a focus on automobile parts. Up until the mid-1990s, such applications were examined through testing conducted within the range of stress that would not cause parts to fail. Subsequently, methods designed to take fracturing into consideration were used for energy-absorbing rib structures. Although the plastic strain at failure was treated as a constant because computer performance was poor back then, an adequate accuracy was still achieved at a practical level (**Fig. 9**).

The plastic strain at failure was determined in the following manner: First, the result of the crash test using the specified evaluation sample was compared to that of the reproduction analysis of the crash test, for which the plastic strain at failure was tentatively determined as a parameter; and subsequently the plastic strain at failure was determined in such a manner that the deformation behavior observed during the crash test and that observed during the reproduction analysis would coincide. This procedure can be conducted automatically through the application of CAO technology. More specifically, the plastic strain at failure used for impact analysis was deemed to be the design variable, and the time average of the square of the acceleration difference of the test result and analysis result at the same time on the acceleration-time curve was deemed to be the evaluation function. Subsequently, optimization was conducted in order to obtain a design variable that allowed the evaluation function to be the smallest. Additionally, the Response Surface Method, which is an approximation method, and the Modified Method of Feasible Directions based on the gradient method were used for the optimization algorithm.[47]

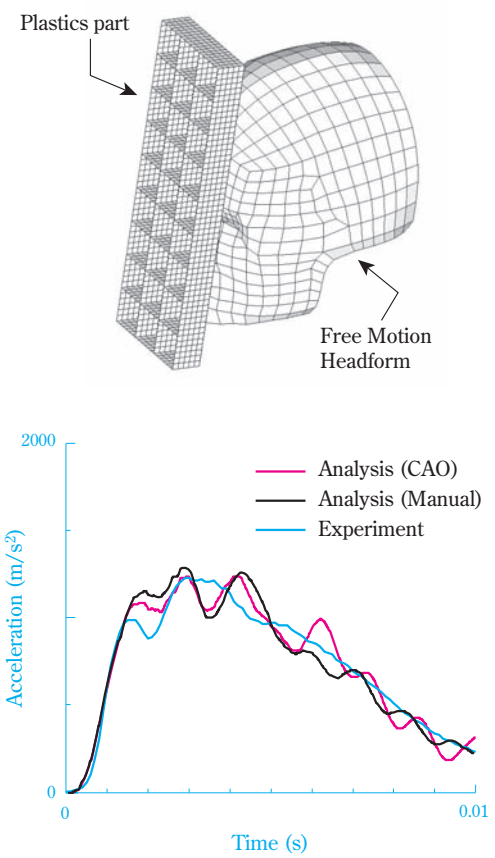

Fig. 9 Example of simulation of impact test for rib box parts

Regarding the CAO technology, the application of quality engineering was also examined, as was the optimization of the impact absorption performance[48], taking into account the dispersion of the impact positions of the impactor.

Furthermore, the methods of impact analysis were investigated for injection molding parts using long

glass fiber reinforced polypropylene and injection foam molded parts. Consequently, a result roughly reflecting the load generated during the crash test was obtained.

(2) Fluid-Structure Interaction and Impact Analysis

For fluid-structure interaction and impact analysis, a drop test using containers filled with liquid (bottles, standing pouches, etc.) and an airbag cover (virtual) deployment test were conducted. Standing pouches used in applications such as containers for detergent refills have a structure in which the side wall is made by affixing two pieces of film at their edges and the bottom surface is made by affixing a film to the side wall.

In the event the heat seal strength is not sufficient when pieces of film are affixed using a heat-seal method, the heat-sealed areas may separate when the object is dropped to the ground. An impact analysis was conducted on a drop test of a standing pouch which had an adhesive strength corresponding to an insufficient heat seal strength. The heat-sealed areas became separated, as seen in the experiment (**Fig. 10**).

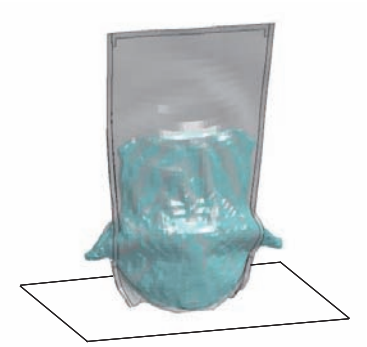

Fig. 10 Example of drop impact analysis for the standing-pouch

An airbag cover that houses an airbag has a thin groove-like area called a “tear line”. When an airbag deploys, the tear line breaks and the airbag cover door opens. Because it is preferable that the airbag cover door will not be blown off upon deployment even at a low temperature, impact analysis was conducted for the (virtual) deployment test at a low temperature.

For materials that show a significant degree of elongation at a low temperature, it is difficult to obtain the strain-rate dependency at region A because the low-speed edge in region A (**Table 1**) is close to the upper limit of the measuring speed of the high-speed tensile testing machine.

Because equation (6), which is used for fitting the yield stress, is binominal, a critical point exists on the curve indicating the strain-rate dependency of the yield stress (**Fig. 11** (a)). Moreover, since this critical point moves from side to side when the temperature changes, and assuming that the time-temperature shift factor of the side-to-side movement coincides with the time-temperature shift factor of the fracture characteristics, the dependence of the nominal strain at break on the nominal strain rate was estimated using the measured values at multiple temperature points (**Fig. 11** (b)).

Regarding two types of materials having different low-temperature performance, the aforementioned dependence of the nominal strain at break on the nominal strain rate was simply converted from the nominal strain to a value equivalent to the true strain. The value thus obtained was then used for the impact analysis of the airbag cover (virtual) deployment test. When performing the impact analysis using the shape of Sumitomo Chemical’s proprietary specimen by setting the test temperature at –35°C, only the airbag

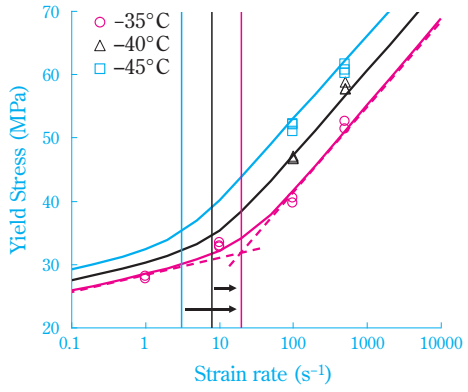

(a) Dependence of nominal yield stress on nominal strain rate

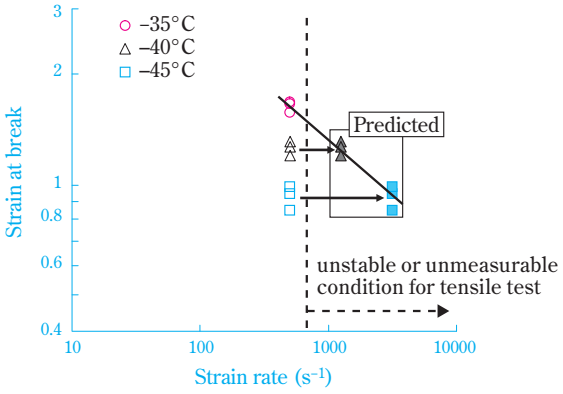

(b) Dependence of nominal strain at break on nominal strain rate

Fig. 11 Determination of failure characteristics

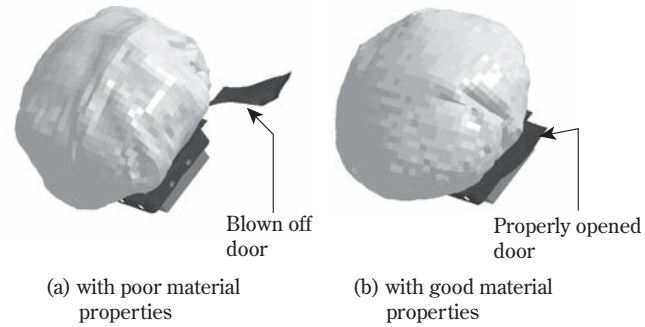

Fig. 12 Airbag cover deployment test analysis result

cover doors which were made of materials having poor low-temperature performance were blown off upon impact (**Fig. 12**).

(3) Effect of Improving the Accuracy of the Elastic-plastic Model

Using an elastic-plastic model, an impact analysis was conducted for the falling weight impact test as shown in **Fig. 13**.

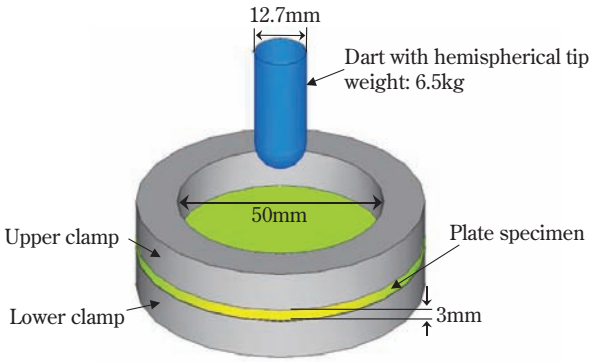

Fig. 13 Schematic diagram of CAE analysis model for the falling weight impact test

The test was conducted using a material model designed in a such manner that the hydrostatic pressure dependence of the yield stress, plastic Poisson's ratio and the damage function were taken into account (Model A) A conventional material model (Model B)—in which the von Mises yield criterion was applied, plastic Poisson's ratio after the occurrence of yielding was set to 0.5.and a damage function was not considered—was also used. For both models, the stress-strain curves used for the impact analysis were determined in such a manner that analysis results for the high-speed tensile test would coincide with the experimental results within a range that would not cause fracture. A two-dimensional axisymmetric model (a certain type of solid model) was used as a finite-element model.

Fig. 14 shows the results of the impact analysis for the falling weight impact test. It is obvious that the prediction accuracy of the experimental data was higher when using Model A as compared to the conventional Model B.

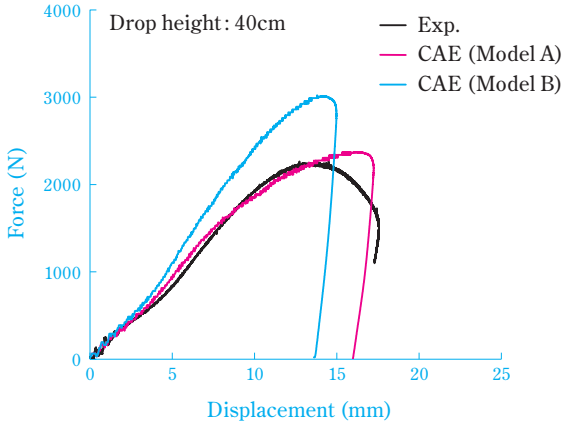

Fig. 14 Comparison of experimental result and CAE predictions for the falling weight impact test

5. Future Prospects

It has been reported that the behavior of materials after reaching the yield point can be explained when assuming rubber elasticity.[49] There is also a report that discusses the relationship between the uniaxial deformation behavior and (strain induced) crystallization/melting behaviors of rubber.[50] Thus, when conducting impact analysis in the field of resins, one can assume that it is ideal to consider the rubber elasticity and crystal morphology of the test material during plastic deformation. Moreover, polymers characteristically generate heat when stretched due to the decrease in entropy (the Gough-Joule effect).[51] Polymers also generate heat due to plastic deformation. It can therefore be assumed that, in order to conduct more realistic impact analysis in the future, it is essential to consider temperature change.

Additionally, multi-scale simulation has garnered attention in recent years. Because crystalline resins form a mixture of crystals and amorphous material, a method to reflect the structure and deformation of the mixed system into the macro-scale structural analysis is now under investigation[52), 53)], and thus its practical application is anticipated.

Regarding the numerical calculation technique, the Extended Finite Element Method (XFEM),[54] by which one can examine the propagation of cracking with high accuracy has garnered attention, as has the particle method which is suitable for the computation of large deformations because the method does not utilize mesh. It is expected that these methods will be applied to plastics CAE.

Conclusion

Given the rapid advancement in computer performance, which has expanded the scale of computation, the input of detailed part information regarding part configurations has become relatively simple. The use of more detailed models is also slowly but surely becoming popular for material models which have seen simplification as one of the results of shorter computation time. Sumitomo Chemical also plans to combine CAE for product design with CAE for polymer design in the future.

References

1) J. R. Lemon, S. K. Tolani and A. L. Klosterman, *CAD-Fachgespräch*, **1980**, 161 (1980).
2) Y. Togawa, T. Hirota and S. Nagaoka, *SUMITOMO KAGAKU*, **2004-Ⅱ**, 15 (2004).
3) S. Masui, Y. Togawa, T. Sakai, T. Kikuchi and N. Usui, *SUMITOMO KAGAKU*, **1984-Ⅱ**, 70 (1984).
4) M. Nagata, T. Kikuchi, Y. Nakamura, Y. Togawa and T. hara, *SUMITOMO KAGAKU*, **1992-Ⅱ**, 68 (1992).
5) Y. Togawa, K. Higashi, M. Tsutsubuchi, T. kayanoki and M. Shimojo, *SUMITOMO KAGAKU*, **1995-Ⅰ**, 75 (1995).
6) S. Nagano, H. Yamauchi and M. Hirakawa, *SUMITOMO KAGAKU*, **2001-Ⅱ**, 13 (2001).
7) M. Tsutsubuchi, T. Kitayama, Y. Togawa, T. Nishio and, H. Kutschera, *Intern. Polym. Process*, **15**(3), 313 (2000).
8) S. Nagaoka, M. Tsutsubuchi and Y. Togawa, *JSPP '98 Symposium Papers*, **1998**, 39.
9) M. Morikawa, Y. Masutani and S. Shiromoto, *SUMITOMO KAGAKU*, **2009-Ⅰ**, 4 (2009).
10) Y. Miyazaki, Seikei-Kakou, **22**(10), 531 (2010).
11) M. Walter, H. Chladek and A. Hus, *4th European LS-DYNA Users Conference*, **2003**, G-1-15.
12) I. Lupea, J. Comier and S. Shah, *8th International LS-DYNA Users Conference*, **2004**, 5-57.
13) T. Yeo and J. Park, *2003 ABAQUS Users' Conference*, **2003**.
14) T. Goel and N. Stander, *Comput. Methods Appl. Mech. Engrg.* **198**, 2137 (2009).
15) M. Keranen, S. Krishnaraj, K. Kulkarni, L. Lu, R. Thyagarajan and V. Ganesan, *SAE Technical Paper*, 2005-01-1221 (2005).
16) C. J. Ribeiro, J.C. Viana, F.Vilaca and J. Azenha, *Plastics, Rubber and Composites*, **35**, 253 (2006).
17) A. Malladi, Saifuddin and G. Gadekar, *SAE Technical Paper*, 2011-26-0014 (2011).
18) T. Yasuno, E. Ichimura, R. Taniguchi, S. Tanaka and M. Yoshida, *JSAE Annual Congress Proceedings*, **No.99-98**, 9 (1998).
19) T. Kondo and T. Yasuki, *JSAE Annual Congress Proceedings*, **No.31-99**, 13 (1999).
20) M. Kanai, K. Shimo, K. Takeuchi, K. Kono and H. Suganuma, *Proceedings of the Kanto Branch Meeting of JSME*, **2006**, 217.
21) H. Mae, *JSME Materials and Processing Division Newsletter*, **32**, 15 (2006).
22) J. M. Lorenzo, *SAE Technical Paper*, 1999-01-0433 (1999).
23) K. Lee, T. Yeo, S. Park, H. A. Gese and H. Dell, *SAE Technical Paper*, 2008-01-1116 (2008).
24) P.A. Du Bois, M. Koesesters, T. Frank and S. Kolling, *3. LS-DYNA Anwenderforum*, **2004**, C-I-1.
25) P.A. Du Bois, S. Kolling, M. Koesters and T. Frank, *International Journal of Impact Engineering*, **32**, 725 (2006).
26) M. C. H. Lee and G. E. Novak, *SAE Technical Paper*, 2006-01-1187 (2006).
27) J. Itoh, X. Li, S. Takada, M. Miyazaki, H. Nishimura and T. Miyashita, *Proceedings of JSME 13th Computational Mechanics Division Conference*, **2000**, 525.
28) D. Yu, J. B. Kwak, S. Park and J. Lee, *Microelectronics Reliability*, **50**, 1028 (2010).
29) K. H. Low, A. Yang, K.H. Hoon, X. Zhang, J. K. T. Lim and K. L. Lim, *Advances in Engineering Software*, **32**, 683 (2001).
30) T. Allen, J. Hart, J. Spurr, S. Haake and S. Goodwill, *Procedia Engineering*, **2**, 3275 (2010).
31) K. Tanaka, Y. Teranishi and S. Ujihashi, *Transactions of the Japan Society of Mechanical Engineers, Series C*, **76**(772), 3343 (2010).
32) W. Petersen and J. McPhee, *Sports Eng.*, **12**(2), 77(2010).
33) A. W. Pugh, R. Hamilton, D. H. Nash and S. R. Otto, *Procedia Engineering*, **2**, 3231 (2010).

34) Y. Kanda, *Transactions of the Japan Society of Mechanical Engineers, Series C*, **65**(638), 3890(1999).
35) H. Akiba and Y. Shibata, *SIMULATION*, **25**(4), 34(2006).
36) S. Matsuoka, "Koubunshi no kanwa-Genshou-Riron, Jikken to Konpyuta de Miru Kougaku-teki-Seishitsu no Kiso" ["Relaxation Phenomena in Polymers -fundamentals of engineering properties with theory, experiment and computer-", First Printing, S. Ichihara, Kodansha Scientific (1995), p. 172.
37) W. Michaeli, M. Glismann, *Polymer Testing*, **20**(5), 591.
38) Y. Tomita, *Journal of the Society of Materials Science, Japan*, **57**(3), 209 (2008) .
39) E.T.J. Klompen, L.E. Govaert, *Mech. Time-depend. Mater.*, **3**, 49 (1999).
40) Y. Sanomura, *Journal of the Society of Materials Science, Japan*, **50**(9), 968 (2001).
41) F. Grytten, H. Daiyan, M. Polanco-Loria and S. Dumoulin, *Polymer Testing*, **28**(6), 653 (2009).
42) V. Delhaye, A. H. Clausen, F. Moussy, R.Othman and O.S.Hopperstad, *International Journal of Impact Engineering*, **38**(4), 208 (2011).
43) A. Sasaki, M. Kuroda, *JSPP '05 Symposium Papers*, **2005**, 189.
44) M. Nutini and M. Vitali, *7. LS-DYNA Anwenderforum*, **2008**, D-I-11.
45) K. Nitta and T Ishiburo, *Kobunshi Kako [Polymer Applications]*, **51**(6), 251 (2002).
46) J. Takahashi, T. Yamamoto, and K Shizawa, *Proceedings of JSME 19th Computational Mechanics Division Conference*, **2006**, 391.
47) Y. Togawa, T. Hirota, M. Nagata and T. Yabe, *JSPP '01 Technical Papers*, **2001**, 35.
48) T. Hirota, Y. Miyaguchi, M. Tsutsubuchi and Y. Togawa, *JSPP '06 Symposium Papers*, **2006**, 233.
49) R. N. Haward, *J. Polym. Sci. Part B:Polymer Physics*, **45**, 1090 (2007).
50) Y. Miyamoto, *Nippon Gomu Kyokaishi*, **77**(1), 12 (2004).
51) S. Murahashi, H. Fujita and S. Nozakura, "Kobunshi Kagaku" ["Macromolecular Chemistry"], third edition, KYORITSU SHUPPAN (1983), p. 288.
52) I. Doghri, "Mechanics of Deformable Solids, Linear and Nonlinear Analytical and Computational Aspects", Springer (2000), p.519.
53) M. Uchida, N. Tada and Y. Tomita, *Transactions of the Japan Society of Mechanical Engineers, Series A*, **77**(778), 902 (2011).
54) N. Moes, J. Dolbow, and T. Belytschko, *International Journal for Numerical Methods in Engineering*, **46**(1), 131 (1999).
55) Y. Sakai and A Yamashita, *Transactions of the Japan Society of Mechanical Engineers, Series A*, **67** (659), 1093 (2001).

PROFILE

Masaaki Tsutsubuchi
Sumitomo Chemical Co., Ltd.
Plastics Technical Center
Senior Research Associate

Yasuhito Niwa
Sumitomo Chemical Co., Ltd.
Plastics Technical Center

Tomoo Hirota
Sumitomo Chemical Co., Ltd.
Plastics Technical Center
Senior Research Associate

Tai Shimasaki
Sumitomo Chemical Co., Ltd.
Plastics Technical Center